Feasibility of Intestinal MR Elastography in Inflammatory Bowel Disease

Rolf Reiter, MD,[1,2*] Florian N. Loch, MD,[3] Carsten Kamphues, MD,[3] Christian Bayerl, MD,[1] Stephan R. Marticorena Garcia, MD,[1] Britta Siegmund, MD,[4] Anja A. Kühl, PhD,[5] Bernd Hamm, MD,[1] Jürgen Braun, PhD,[6] Ingolf Sack, PhD,[1] and Patrick Asbach, MD[1]

Background: While MR enterography allows detection of inflammatory bowel disease (IBD), the findings continue to be of limited use in guiding treatment—medication vs. surgery.
Purpose: To test the feasibility of MR elastography of the gut in healthy volunteers and IBD patients.
Study Type: Prospective pilot.
Population: Forty subjects (healthy volunteers: $n = 20$, 37 ± 14 years, 10 women; IBD patients: $n = 20$ (ulcerative colitis $n = 9$, Crohn's disease $n = 11$), 41 ± 15 years, 11 women).
Field Strength/Sequence: Multifrequency MR elastography using a single-shot spin-echo echo planar imaging sequence at 1.5 T with drive frequencies of 40, 50, 60, and 70 Hz.
Assessment: Maps of shear-wave speed (SWS, in m/s) and loss angle (φ, in rad), representing stiffness and solid–fluid behavior, respectively, were generated using tomoelastography data processing. Histopathological analysis of surgical specimens was used as reference standard in patients.
Statistical Tests: Unpaired t-test, one-way analysis of variance followed by Tukey post hoc analysis, Pearson's correlation coefficient and area under the receiver operating characteristic curve (AUC) with 95%-confidence interval (CI). Significance level of 5%.
Results: MR elastography was feasible in all 40 subjects (100% technical success rate). SWS and φ were significantly increased in IBD by 21% and 20% (IBD: 1.45 ± 0.14 m/s and 0.78 ± 0.12 rad; healthy volunteers: 1.20 ± 0.14 m/s and 0.65 ± 0.06 rad), whereas no significant differences were found between ulcerative colitis and Crohn's disease ($P = 0.74$ and 0.90, respectively). In a preliminary assessment, a high diagnostic accuracy in detecting IBD was suggested by an AUC of 0.90 (CI: 0.81–0.96) for SWS and 0.84 (CI: 0.71–0.95) for φ.
Data Conclusion: In this pilot study, our results demonstrated the feasibility of MR elastography of the gut and showed an excellent diagnostic performance in predicting IBD.
Evidence Level: 1
Technical Efficacy: Stage 1

J. MAGN. RESON. IMAGING 2022;55:815–822.

Despite the success of standard clinical MR enterography in detecting inflammatory bowel disease (IBD), its role in providing therapeutic guidance remains limited.[1–3] While fibrotic bowel strictures require surgery or endoscopic intervention, patients with inflammatory bowel strictures may benefit from anti-inflammatory drug treatment.[1] Therefore, characterization of stricturing lesions is crucial for therapeutic decision-making and monitoring the treatment response over

View this article online at wileyonlinelibrary.com. DOI: 10.1002/jmri.27833

Received Apr 30, 2021, Accepted for publication Jun 25, 2021.

*Address reprint requests to: R.R., Hindenburgdamm 30, 12203 Berlin, Germany. E-mail: rolf.reiter@charite.de

From the [1]Department of Radiology, Charité – Universitätsmedizin Berlin, Corporate Member of Freie Universität Berlin and Humboldt-Universität zu Berlin, Hindenburgdamm 30, Berlin, 12203, Germany; [2]Berlin Institute of Health (BIH), Anna-Louisa-Karsch-Str. 2, Berlin, 10178, Germany; [3]Department of Surgery, Charité – Universitätsmedizin Berlin, Corporate Member of Freie Universität Berlin and Humboldt-Universität zu Berlin, Hindenburgdamm 30, Berlin, 12203, Germany; [4]Department of Gastroenterology, Infectious Disease, Rheumatology, Charité – Universitätsmedizin Berlin, Corporate Member of Freie Universität Berlin and Humboldt-Universität zu Berlin, Hindenburgdamm 30, Berlin, 12203, Germany; [5]iPATH.Berlin-Immunopathology for Experimental Models, Core Facility, Charité – Universitätsmedizin Berlin, Corporate Member of Freie Universität Berlin and Humboldt-Universität zu Berlin, Hindenburgdamm 30, Berlin, 12203, Germany; and [6]Department of Medical Informatics, Charité – Universitätsmedizin Berlin, Corporate Member of Freie Universität Berlin and Humboldt-Universität zu Berlin, Hindenburgdamm 30, Berlin, 12203, Germany

time. In current MRI protocols, detection of active inflammation is mainly based on a qualitative interpretation of T2-weighted fat-saturated images with high signal intensities indicating edema, whereas no reliable imaging marker of fibrosis has been established.[1] So far, noninvasive imaging tests lack accuracy to guide clinical decisions.[1,2] Endoscopy with histopathological assessment of biopsies remains the diagnostic reference standard.[1,2] Yet endoscopy also has several limitations, including reliance on a superficial inspection of the mucosa, lack of depth of biopsies and sampling errors due to a heterogeneous distribution of inflammation in Crohn's disease.[4] The lack of an accurate noninvasive diagnostic test restricts patient management, therapy monitoring and stratification in clinical trials. Noninvasive surrogate markers are warranted to replace invasive diagnostic procedures.[5–7]

MR elastography is a noninvasive quantitative imaging method to assess viscoelastic tissue properties.[8–12] One of its main applications so far has been the assessment of hepatic fibrosis[13–16] and, more recently, hepatic inflammation.[17–19] Moreover, technical advances have improved the spatial resolution and noise robustness of elastograms, allowing the examination of smaller organs such as the prostate[10,20] and pancreas.[21,22]

For the investigation of IBD, a few ultrasound-based elastography studies have been performed in animal models and humans.[23–25] Thus, the aim of this study was to investigate the feasibility of MR elastography of the gut in healthy volunteers and IBD patients using histopathological analysis of surgical specimens as reference standard.

Materials and Methods

Subjects

The study was approved by the local institutional review board, and all subjects gave informed oral and written consent. Between July 2019 and December 2020, a total of 40 subjects were investigated in this prospective single-center study, including 20 healthy volunteers and 20 patients with IBD (ulcerative colitis $n = 9$, Crohn's disease $n = 11$). Inclusion criteria for patients were clinically established diagnosis of either ulcerative colitis or Crohn's disease with scheduled and clinically indicated surgery and age ≥ 18 years. The diagnosis of ulcerative colitis or Crohn's disease was reported using the Montreal classification and confirmed using histopathological analysis of surgical specimens as reference standard.[26] Exclusion criteria were other concurrent bowel diseases, fecal impaction, increased peristalsis, and general MRI contraindications.

MR Elastography

Multifrequency MR elastography with tomoelastography processing was performed at 1.5 T (Magnetom Aera, Siemens Healthineers, Erlangen, Germany) with an 18-channel phased-array coil in combination with the spine-array coil. Mechanical frequencies of 40, 50,

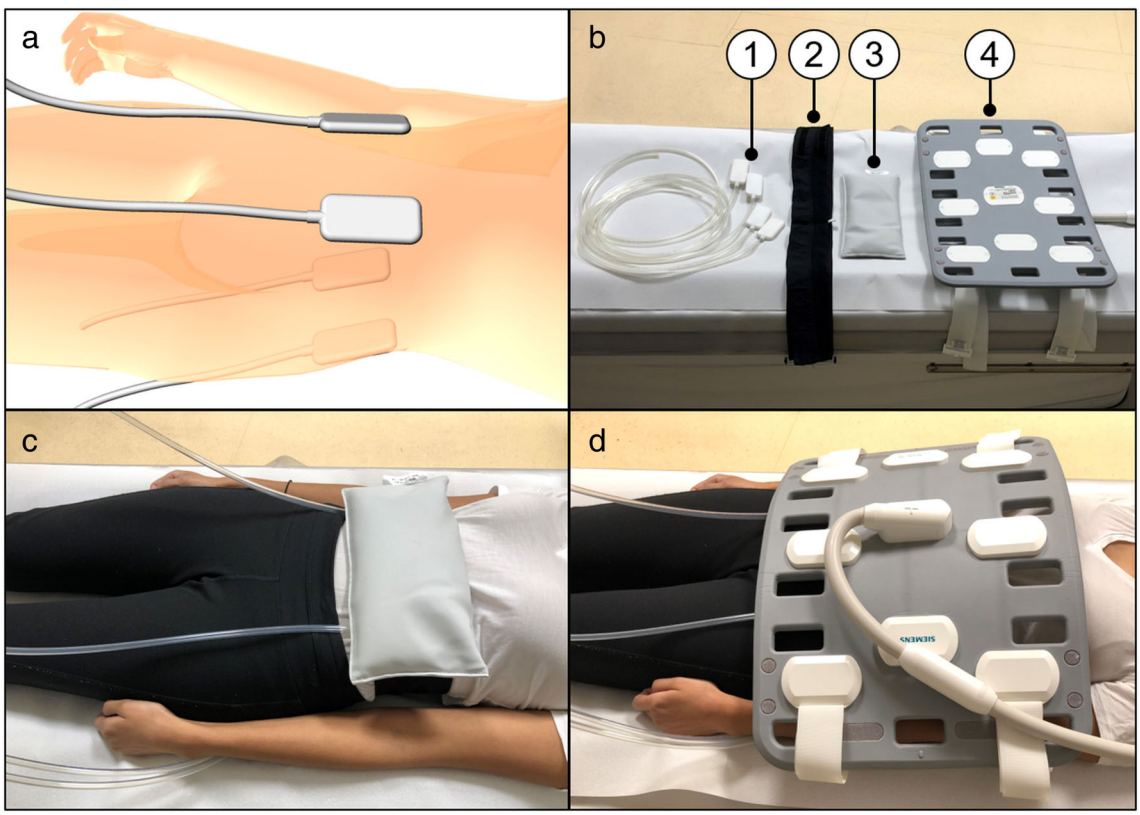

FIGURE 1: MR elastography setup. (a) Schematic overview: two drivers in anterior and two drivers in posterior position. (b) Overview of components: drivers with hoses (1), belt with pockets for driver positioning (2), sand-filled cushion (3), MRI phased-array coil (4). (c) and (d) show the setup at the lower abdomen in a volunteer.

60, and 70 Hz were generated using four drivers with compressed-air hoses and bulge outlets. These drivers were placed around the lower abdomen with two drivers in anterior and two drivers in posterior position (Fig. 1). Additionally, a sand-filled cushion was placed above the anterior driver for optimal wave transmission to the gut. More details about the MR elastography setup and hardware can be found in the studies by Shahryari et al[12] and Hudert et al.[27] The 3D wave fields were acquired using a single-shot spin-echo echo planar imaging sequence,[28] and imaging was performed for a total of 5:17 min with patients breathing freely.[29] MR elastography scan parameters were as follows: 25 axial slices, 8 time steps, 100 × 66 matrix, 3 × 3 × 5 mm^3 resolution, repetition time of 3070 msec, and echo time of 50 msec. Additionally, a conventional axial and coronal T2-weighted half-Fourier acquisition single-shot turbo spin-echo sequence was acquired to plan elastograms and to ensure the inclusion of IBD lesions. To facilitate comparison of patients and healthy volunteers in this explorative study and for ethical reasons, imaging was performed without active colonic distension with water enema and without administration of oral and intravenous contrast agent or antispasmodic medication.

For preliminary assessment of the reproducibility of gut MR elastography, the entire protocol was repeated five times separated by an hour in one healthy volunteer. The volunteer left and re-entered the scanner room, and the equipment was set up anew for each examination.

Data Processing

The multifrequency processing pipeline provides maps of shear-wave speed (SWS in m/s) as a surrogate of stiffness[30] and loss angle of the complex modulus (φ in rad) as a surrogate of solid–fluid behavior.[31,32] Combination of these two viscoelastic parameters has been previously proposed for the investigation of the liver,[12] kidney,[33] and prostate.[10] φ ranges from 0 rad for pure solids to $\pi/2$ rad for pure fluids and is based on multifrequency dual elasto-visco (MDEV) inversion,[9–12] whereas SWS is based on *k*-MDEV inversion.[8] The algorithm is publicly available at https://bioqicapps.charite.de. An experiment was considered to be technically successful when intestine was visually perceptible on SWS maps. Volumes of interest were manually drawn by a radiologist (R.R., 10 years of experience in abdominal MR elastography) based on SWS maps.

TABLE 1. Demographics of Subjects

	Healthy Volunteers	IBD Patients
Number of subjects	20	20
Female (%)	50	55
Age (y)	37.0 (13.5)	41.4 (14.7)
Body mass index (kg/m^2)	22.0 (2.6)	24.3 (5.2)
C-reactive protein (cutoff for normality <0.5)	-	65.3 (75.4)
Disease duration (months)	-	194.9 (146.6)

Data are means, if not otherwise specified, and numbers in parentheses are standard deviations.
IBD = inflammatory bowel disease.

Statistical Methods

Continuous variables and group values are reported as means and standard deviation. Groups were compared using an unpaired t-test and one-way analysis of variance followed by Tukey post hoc analysis. Pearson's correlation coefficient (*R*) was calculated for MR elastography parameters in relation to age and body mass index. Area under the receiver operating characteristic curve (AUC) analysis with 95%-confidence interval (CI) was used to preliminarily assess the diagnostic accuracy of SWS and φ in predicting IBD. To assess inter-reader agreement, all cases have been reevaluated by a second radiologist (C.B., 5 years of experience in abdominal MR elastography) and intraclass correlation (ICC) with CI has been determined. ICCs were classified as follows: <0.5 defined as poor, 0.5–0.75 defined as moderate, 0.75–0.9 defined as good, and 0.9–1 defined as excellent. The significance level was set to 5%. Statistical analysis was performed in RStudio (version 1.3.1093; R-Foundation, Vienna, Austria).

Results

Demographics of all subjects are listed in Table 1 and medical characteristics of patients are listed in Table 2. All patients were investigated within a median of 1 day (interquartile range, 0) before surgery. MR elastography of the gut was successfully completed in all 40 subjects (100% technical success rate). Representative examples are shown in Fig. 2. The mean volume of interest was 47.4 ± 29.9 cm^3 with a mean number of slices of 17 ± 7. Five hourly repeated scans in one healthy volunteer revealed a low intraindividual standard deviation for both SWS (1.05 ± 0.03 m/s) and φ (0.57 ± 0.03 rad), demonstrating reproducibility. No significant correlation was found between MR elastography parameters (SWS and φ) and age ($P = 0.57$ and 0.43, respectively) or body mass index ($P = 0.84$ and 0.11, respectively). Both SWS and φ were significantly increased in IBD by 21% and 20%, respectively, (all IBD patients [$n = 20$]: 1.45 ± 0.14 m/s and 0.78 ± 0.12 rad vs. healthy volunteers [$n = 20$]: 1.20 ± 0.14 m/s and 0.65 ± 0.06 rad; Fig. 3), whereas no significant differences were found between ulcerative colitis and Crohn's disease (ulcerative colitis [$n = 9$]: 1.43 ± 0.17 m/s and 0.79 ± 0.09 rad vs. Crohn's disease [$n = 11$]: 1.48 ± 0.12 m/s and 0.77 ± 0.15 rad; $P = 0.74$ and 0.90, respectively). Preliminary diagnostic accuracy for the prediction of IBD was calculated with an AUC of 0.90 (CI: 0.81–0.96) for SWS and 0.84 (CI: 0.71–0.95) for φ. Inter-reader agreement was good for SWS with an ICC of 0.78 (CI: 0.62–0.88) and moderate for φ with an ICC of 0.61 (CI: 0.36–0.77).

TABLE 2. Medical Characteristics of Patients

Medical Characteristics	Ulcerative Colitis ($n = 9$)	Crohn's Disease ($n = 11$)
	Number of patients	
Montreal classification age group		
A1, <16 years at diagnosis	0	1
A2, 17–40 years at diagnosis	7	8
A3, >40 years at diagnosis	2	2
Montreal classification disease extent (UC)		
Ulcerative proctitis	0	-
Left-sided UC (distal UC)	4	-
Extensive UC (pancolitis)	5	-
Montreal classification disease extent (CD)		
L1, terminal ileum	-	7
L2, colon	-	2
L3, ileocolon	-	2
+L4, upper gastrointestinal tract disease present	-	0
Montreal classification disease behavior (CD)		
B1, Nonstricturing, nonpenetrating	-	2
B2, Stricturing	-	5
B3, Penetrating	-	4
+B3p, Perianal penetrating	-	0
Montreal classification perianal disease modifier (CD)		
No perianal disease	-	9
Perianal disease present	-	2
Inflammatory bowel disease medication history		
Corticosteroids	5	3
Mesalazine	3	0
Infliximab	1	2
Adalimumab	1	2
Ustekinumab	1	0
Sulfasalazine	1	0
Vedolizumab	1	0
Tacrolimus	1	0
Mercaptopurine	1	0
Azathioprine	0	4
Surgical procedure		
Colectomy	9	2

TABLE 2. Continued

Medical Characteristics	Ulcerative Colitis ($n = 9$)	Crohn's Disease ($n = 11$)
Ileocecal resection	0	9
Indications for surgery		
Failed medical therapy	9	11
Stricture	0	5
Penetrating disease	0	4

UC = ulcerative colitis; CD = Crohn's disease.

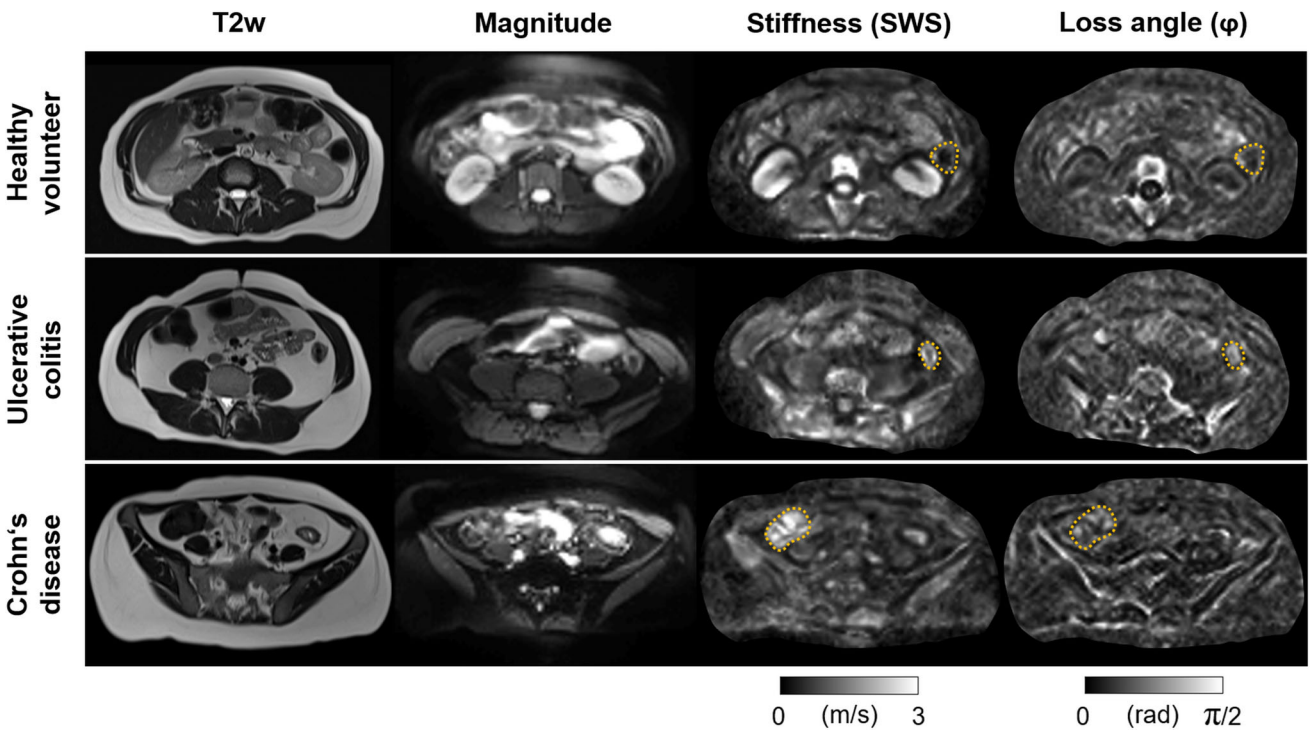

FIGURE 2: Representative examples. Upper row: Healthy volunteer with shear-wave speed (SWS) of 1.09 ± 0.28 m/s and loss angle (φ) of 0.59 ± 0.20 rad in the descending colon. Middle row: Patient with ulcerative colitis-based lesion in the descending colon with SWS of 1.58 ± 0.36 ms and φ of 0.88 ± 0.31 rad. Lower row: patient with Crohn's disease-based lesion in the ileocecal junction with SWS of 1.79 ± 0.39 ms and φ of 0.73 ± 0.22 rad. The increased viscoelasticity measured in both patients are visually perceptive on SWS and φ maps.

Discussion

This explorative study investigated MR elastography of the gut in healthy volunteers and IBD patients using histopathological analysis of surgical specimens as reference. Anatomical details such as the colon and ileum were visually perceptible on both SWS and φ maps, eliminating the need for superimposition of morphological images. The 100% technical success rate we achieved in healthy volunteers and patients, the low standard deviation of repeated measurements and the good inter-reader agreement for SWS confirm the feasibility of the method. In our study, we found significantly increased values for both SWS and φ in IBD compared to healthy volunteers, whereas no differences were evident between ulcerative colitis and Crohn's disease. Age and body mass index did not affect MR elastography parameters, which facilitates potential clinical application of the method. Our preliminary results also showed an excellent diagnostic performance in predicting IBD for both SWS and φ.

These results support previous evidence from a case report using MR elastography, which found an SWS of 1.47 ± 0.28 m/s and φ of 0.80 ± 0.11 rad in a patient

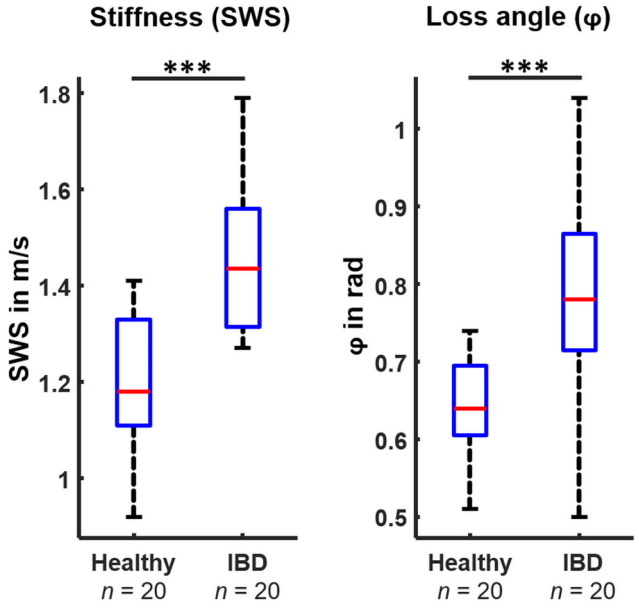

FIGURE 3: Boxplots display median, upper and lower quartiles, and whiskers of shear-wave speed (SWS) and loss angle (φ). Statistically significant differences are indicated by asterisks (***) for $P < 0.001$. IBD = inflammatory bowel disease.

with acute appendicitis after antibiotic treatment.[34] A few ultrasound-based elastography pilot and proof-of-concept studies with histopathological correlation have shown similar biomechanical endpoints as our study. For instance, Stidham et al distinguished inflammatory vs. fibrotic gut in a rat model of IBD using normalized strain measurements (−2.07 vs. −1.10; $P = 0.037$).[23] In the same study, the authors were able to distinguish stenotic vs. adjacent normal small bowel in seven patients with Crohn's disease (−0.87 vs. −1.99; $P = 0.0008$).[23] Baumgart et al detected fibrotic gut tissue in stricturing Crohn's disease in a group of 10 patients.[24] They found an increased strain ratio in unaffected vs. affected gut segments using real-time elastography (169.0 ± 27.9 vs. 43.0 ± 25.9, $P < 0.001$) and tensiometry (77.1 ± 21.4 vs. 13.3 ± 11.2, $P < 0.001$). Additionally, they showed an association between strain measurements and collagen deposition in fibrosis. In contrast, Serra et al found no correlation between the strain ratio and fibrosis ($P = 0.87$) or inflammation ($P = 0.53$) in 26 patients with Crohn's disease.[25] Also, other quantitative MRI techniques have shown promising results. For instance, Li et al showed that magnetization transfer MRI outperformed diffusion and contrast-enhanced imaging in assessing varying degrees of bowel fibrosis with or without coexisting inflammation in Crohn's disease.[35]

Clinical MR enterography for the detection of strictures has been investigated in several studies using histopathological reference. One of the largest series included 49 patients with Crohn's disease and was performed by Sinha et al.[36] For the detection of all abnormal segments, they found AUC values as follows: 0.96 for mural thickness, 0.81 for the enhancement ratio of the abnormal bowel, and 0.68 for the mesentery enhancement ratio. Rimola et al were able to differentiate low vs. moderate/severe inflammation and mild/moderate vs. severe fibrosis in a study including 41 patients with Crohn's disease.[37] They showed that fibrosis was associated with the percentage of enhancement gain, which discriminated mild/moderate vs. severe fibrosis with an AUC of 0.93. Moreover, several semiquantitative MRI scores have been proposed to predict active disease.[38–40] The Magnetic Resonance Index of Activity score was developed in 50 patients with Crohn's disease examined by ileocolonoscopy. Based on wall thickness, relative contrast enhancement, presence of edema and presence of ulcers, their model achieved an AUC of 0.89.[38,39] The Acute Inflammation Score was developed in 16 patients with Crohn's disease and elective small bowel surgical resection.[40] It is based on the qualitative scoring (0–3) of mural thickness and T2 signal. Their model, applied to 26 patients with endoscopic biopsies, achieved an AUC of 0.77.

While MR enterography studies have shown good performance in detecting strictures and in evaluating the degree of inflammation, characterization of intestinal fibrosis remains challenging. Based on a biomechanical-based contrast mechanism, our pilot study results showed a similar diagnostic performance to the above-mentioned MR enterography studies for the detection of IBD, while no oral or intravenous contrast agent, no active colonic distension with water enema and no antispasmodic agents were administered. Moreover, current MR enterography protocols and scores rely on a combination of pulse sequences, contrast agents and subjective image interpretation. Therefore, our results motivate further investigation of MR elastography of the gut as a short adjunct sequence to supplement current MR enterography protocols. Especially, the diagnostic performance for the quantification of fibrosis and inflammation as well as the influence of bowel mater, bowel preparation with oral contrast agents and physiological changes to viscoelastic properties of the gut should be investigated in the future.

Limitations

Only a small number of subjects were investigated in our pilot study. All patients included were scheduled for elective surgery the following day, which preselected patients with rather pronounced fibrosis and low inflammatory activity. Therefore, an in-depth assessment of fibrotic and inflammatory components was not performed in this initial study. However, histopathological analysis of surgical specimens is the best reference standard available, and a strength of this study is the short interval between MR elastography and surgery, which allows close correlation of findings.

Conclusion

Our pilot results demonstrated the feasibility of MR elastography of the gut and showed excellent diagnostic performance in predicting IBD. This study provides basic data for the biophysical characterization of intestinal fibrosis and inflammation in IBD in the future.

Acknowledgments

Preliminary results of this work were presented at the Annual Meeting of the International Society for Magnetic Resonance in Medicine in 2020. This study was funded by the Deutsche Forschungsgemeinschaft (DFG, German Research Foundation): RE 4161/2-1 (Rolf Reiter); SFB 1340/1 "Matrix in Vision", project number 372486779 (Bernd Hamm, Jürgen Braun, Ingolf Sack, Patrick Asbach, Anja A. Kühl and Britta Siegmund) and GRK 2260 BIOQIC (Ingolf Sack, Jürgen Braun). Rolf Reiter is a participant of the BIH-Charité Digital Clinician Scientist Program funded by the Charité – Universitätsmedizin Berlin and the Berlin Institute of Health and the DFG. Open Access funding enabled and organized by Projekt DEAL.

References

1. Maaser C, Sturm A, Vavricka SR, et al. ECCO-ESGAR guideline for diagnostic assessment in IBD part 1: Initial diagnosis, monitoring of known IBD, detection of complications. J Crohns Colitis 2019;13:144-164.
2. Sturm A, Maaser C, Calabrese E, et al. Ecco-esgar guideline for diagnostic assessment in ibd part 2: Ibd scores and general principles and technical aspects. J Crohns Colitis 2019;13:273-284.
3. Bruining DH, Zimmermann EM, Loftus EV, Sandborn WJ, Sauer CG, Strong SA. Consensus recommendations for evaluation, interpretation, and utilization of computed tomography and magnetic resonance Enterography in patients with small bowel Crohn's disease. Radiology 2018;286:776-799.
4. Bettenworth D, Bokemeyer A, Baker M, et al. Assessment of Crohn's disease-associated small bowel strictures and fibrosis on cross-sectional imaging: A systematic review. Gut 2019;68:1115-1126.
5. Zhang TT, Chang W, Wang ZJ, Sun DC, Ohliger MA, Yeh BM. Bowel wall visualization using MR Enterography in relationship to bowel lumen contents and patient demographics. J Magn Reson Imaging 2021;54: 728-736.
6. Scott RA, Williams HG, Hoad CL, et al. MR measures of small bowel wall T2 are associated with increased permeability. J Magn Reson Imaging 2021;53:1422-1431.
7. Cruz-Romero C, Guo A, Bradley WF, Vicentini JRT, Yajnik V, Gee MS. Novel associations between genome-wide single nucleotide polymorphisms and MR Enterography features in Crohn's disease patients. J Magn Reson Imaging 2021;53:132-138.
8. Tzschätzsch H, Guo J, Dittmann F, et al. Tomoelastography by multifrequency wave number recovery from time-harmonic propagating shear waves. Med Image Anal 2016;30:1-10.
9. Streitberger K-J, Lilaj L, Schrank F, et al. How tissue fluidity influences brain tumor progression. Proc Natl Acad Sci 2020;117:128-134.
10. Asbach P, Ro S, Aldoj N, et al. In vivo quantification of water diffusion, stiffness, and tissue fluidity in benign prostatic hyperplasia and prostate Cancer. Invest Radiol 2020;55:524-530.
11. Guo J, Bertalan G, Meierhofer D, et al. Brain maturation is associated with increasing tissue stiffness and decreasing tissue fluidity. Acta Biomater 2019;99:433-442.
12. Shahryari M, Tzschätzsch H, Guo J, et al. Tomoelastography distinguishes noninvasively between benign and malignant liver lesions. Cancer Res 2019;79:5704-5710.
13. Reiter R, Tzschätzsch H, Schwahofer F, et al. Diagnostic performance of tomoelastography of the liver and spleen for staging hepatic fibrosis. Eur Radiol 2020;30:1719-1729.
14. Singh S, Venkatesh SK, Wang Z, et al. Diagnostic performance of magnetic resonance elastography in staging liver fibrosis: A systematic review and meta-analysis of individual participant data. Clin Gastroenterol Hepatol 2015;13:440-451.
15. Huwart L, Sempoux C, Salameh N, et al. Liver fibrosis: Noninvasive assessment with MR elastography versus aspartate aminotransferase–to-platelet ratio index. Radiology 2007;245:458-466.
16. Hudert CA, Tzschätzsch H, Rudolph B, et al. How histopathologic changes in pediatric nonalcoholic fatty liver disease influence in vivo liver stiffness. Acta Biomater 2021;123:178-186.
17. Yin M, Glaser KJ, Manduca A, et al. Distinguishing between hepatic inflammation and fibrosis with MR elastography. Radiology 2017;284:694-705.
18. Leitão HS, Doblas S, Garteiser P, et al. Hepatic fibrosis, inflammation, and steatosis: Influence on the MR viscoelastic and diffusion parameters in patients with chronic liver disease. Radiology 2017;283:98-107.
19. Sinkus R, Lambert S, Abd-Elmoniem KZ, et al. Rheological determinants for simultaneous staging of hepatic fibrosis and inflammation in patients with chronic liver disease. NMR Biomed 2018;31:e3956. https://doi.org/10.1002/nbm.3956.
20. Reiter R, Majumdar S, Kearney S, et al. Prostate cancer assessment using MR elastography of fresh prostatectomy specimens at 9.4 T. Magn Reson Med 2019;84:396-404.
21. Zhu L, Guo J, Jin Z, et al. Distinguishing pancreatic cancer and autoimmune pancreatitis with in vivo tomoelastography. Eur Radiol 2021;31:3366-3374.
22. Marticorena Garcia SR, Zhu L, Gültekin E, et al. Tomoelastography for measurement of tumor volume related to tissue stiffness in pancreatic ductal adenocarcinomas. Invest Radiol 2020;55:769-774.
23. Stidham RW, Xu J, Johnson LA, et al. Ultrasound elasticity imaging for detecting intestinal fibrosis and inflammation in rats and humans with Crohn's disease. Gastroenterology 2011;141:819-826.
24. Baumgart DC, Müller HP, Grittner U, et al. US-based real-time elastography for the detection of fibrotic gut tissue in patients with stricturing Crohn disease. Radiology 2015;275:889-899.
25. Serra C, Rizzello F, Pratico C, et al. Real-time elastography for the detection of fibrotic and inflammatory tissue in patients with stricturing Crohn's disease. J Ultrasound 2017;20:273-284.
26. Silverberg MS, Satsangi J, Ahmad T, et al. Toward an integrated clinical, molecular and serological classification of inflammatory bowel disease: Report of a working party of the 2005 Montreal world congress of gastroenterology. Can J Gastroenterol 2005;19:5A-36A. https://doi.org/10.1155/2005/269076.
27. Hudert CA, Tzschätzsch H, Rudolph B, et al. Tomoelastography for the evaluation of pediatric nonalcoholic fatty liver disease. Invest Radiol 2019;54:198-203.
28. Dittmann F, Hirsch S, Tzschätzsch H, Guo J, Braun J, Sack I. In vivo wideband multifrequency MR elastography of the human brain and liver. Magn Reson Med 2016;76:1116-1126.
29. Shahryari M, Meyer T, Warmuth C, et al. Reduction of breathing artifacts in multifrequency magnetic resonance elastography of the abdomen. Magn Reson Med 2021;85:1962-1973.
30. Dittmann F, Tzschätzsch H, Hirsch S, et al. Tomoelastography of the abdomen: Tissue mechanical properties of the liver, spleen, kidney, and pancreas from single MR elastography scans at different hydration states. Magn Reson Med 2017;78:976-983.
31. Hirsch S, Guo J, Reiter R, et al. MR elastography of the liver and the spleen using a piezoelectric driver, single-shot wave-field acquisition, and multifrequency dual parameter reconstruction. Magn Reson Med 2014;71:267-277.
32. Streitberger K-J, Reiss-Zimmermann M, Freimann FB, et al. High-resolution mechanical imaging of glioblastoma by multifrequency magnetic resonance elastography. PLoS One 2014;9:e110588. https://doi.org/10.1371/journal.pone.0110588.
33. Lang ST, Guo J, Bruns A, et al. Multiparametric quantitative MRI for the detection of IgA nephropathy using tomoelastography, DWI, and BOLD imaging. Invest Radiol 2019;54:669-674.
34. Marticorena Garcia SR, Hamm B, Sack I. Tomoelastography for noninvasive detection and treatment monitoring in acute appendicitis. BMJ Case Rep 2019;12:e230791. https://doi.org/10.1136/bcr-2019-230791.

35. Li X, Mao R, Huang S, et al. Characterization of degree of intestinal fibrosis in patients with Crohn disease by using magnetization transfer MR imaging. Radiology 2018;287:494-503.

36. Sinha R, Murphy P, Sanders S, et al. Diagnostic accuracy of high-resolution MR enterography in Crohn's disease: Comparison with surgical and pathological specimen. Clin Radiol 2013;68:917-927.

37. Rimola J, Planell N, Rodríguez S, et al. Characterization of inflammation and fibrosis in Crohn's disease lesions by magnetic resonance imaging. Am J Gastroenterol 2015;110:432-440.

38. Rimola J, Rodriguez S, Garcia-Bosch O, et al. Magnetic resonance for assessment of disease activity and severity in ileocolonic Crohn's disease. Gut 2009;58:1113-1120.

39. Rimola J, Ordás I, Rodriguez S, et al. Magnetic resonance imaging for evaluation of Crohn's disease. Inflamm Bowel Dis 2011;17:1759-1768.

40. Steward MJ, Punwani S, Proctor I, et al. Non-perforating small bowel Crohn's disease assessed by MRI enterography: Derivation and histopathological validation of an MR-based activity index. Eur J Radiol 2012;81:2080-2088.